Available online at www.sciencedirect.com
SCIENCE DIRECT®
Organic Electronics 4 (2003) 113–121
Organic Electronics
www.elsevier.com/locate/orgel

High efficiency molecular organic light-emitting diodes based on silole derivatives and their exciplexes

Leonidas C. Palilis [a,1], Hideyuki Murata [b], Manabu Uchida [c], Zakya H. Kafafi [a,*]

[a] Optical Sciences Division, US Naval Research Laboratory, Washington, DC 20375, USA
[b] School of Materials Science, Japan Advanced Institute of Science Technology, Ishikawa 923-1292, Japan
[c] Chisso Corporation, Yokohama, Kanagawa 236-8605, Japan

Abstract

Here, we report the performance of molecular organic light-emitting diodes (MOLEDs) using novel fluorescent silole derivatives as highly efficient blue and green-emitting organic materials. Three silole derivatives, namely 2,5-di-(3-biphenyl)-1,1-dimethyl-3,4-diphenylsilacyclopentadiene (PPSPP), 9-silafluorene-9-spiro-1′-(2′,3′,4′,5′-tetraphenyl)-1′H-silacyclopentadiene (ASP) and 1,2-bis(1-methyl-2,3,4,5,-tetraphenylsilacyclopentadienyl)ethane (2PSP), with high solid-state photoluminescence (PL) quantum yields of 0.85, 0.87 and 0.94, respectively, were used as emissive materials. Another high electron mobility silole derivative, 2,5-bis(2′,2″-bipyridin-6-yl)-1,1-dimethyl-3,4-diphenylsilacyclopentadiene (PyPySPyPy), was used as the electron transport material. MOLEDs using these siloles as emitters and *N*,*N*′-diphenyl-*N*,*N*′-(2-napthyl)-(1,1′-phenyl)-4,4′-diamine (NPB) or *N*,*N*′-diphenyl-*N*,*N*′-bis(3-methylphenyl)-1,1′-biphenyl-4,4′diamine (TPD) as the hole transport material show low operating voltages of 4–4.5 V at a luminance of 100 cd/m^2 and high external electroluminescence (EL) quantum efficiencies of 3.4–4.1% at ~100 A/m^2. MOLEDs based on PPSPP and PyPySPyPy exhibit red-shifted EL spectra which are assigned to exciplexes formed at the interface between the hole transporting layer NPB or TPD and the PPSPP or PyPySPyPy light-emitting layer, respectively.

1. Introduction

Significant progress in the field of molecularly based organic light-emitting diodes (MOLEDs) has been made since the first report of Tang and Van Slyke [1]. The design of new emissive and charge transport molecular materials has resulted in high performance MOLEDs that are approaching the standards required for display applications [2–4]. However, new materials and device architectures aimed for further improvements in device efficiency, lifetime and operating voltage are continuously being sought in different laboratories worldwide. High device efficiency and low operating voltage are particularly desirable for high performance MOLEDs in display and solid-state lighting applications [5]. The device electroluminescence quantum efficiency is proportional to (and therefore can be limited by) the solid-state photoluminescence (PL) quantum yield (Φ_{PL}) of the emitting molecule, if balanced charge injection and transport can be achieved. On the other hand, to achieve low operating voltage, ohmic charge

* Corresponding author.
E-mail addresses: leonidas@ccs.nrl.navy.mil (L.C. Palilis), kafafi@ccf.nrl.navy.mil (Z.H. Kafafi).
[1] Also at SFA Inc., Largo, MD 20774, USA.

1566-1199/$ - see front matter © 2003 Elsevier B.V. All rights reserved.
doi:10.1016/j.orgel.2003.08.006

injection and fast non-dispersive charge transport are needed. Unfortunately, most organic neat films have low solid-state PL quantum yields as intermolecular interactions and molecular packing usually result in strong luminescence quenching. Also, most organics have low electron mobilities and small solid-state electron affinities since they preferentially transport holes. Therefore, the development of highly emissive materials with large solid-state PL quantum yields as well as high electron affinity electron transport materials are most desirable. One of the more widely used emissive/electron transporting molecules is tris-(8-hydroxyquinolinato) aluminum (Alq_3). It has, however, a low PL quantum yield of $\sim$0.25 [6] and a rather low electron mobility of $\sim 10^{-6}$ cm^2/V s [7]. Doping of an organic host with a highly efficient fluorescent [8] or phosphorescent guest [9] has been employed to take advantage of the high molecular Φ_{PL}. Improvements in the solid-state Φ_{PL} have been achieved via energy transfer from the host to the guest molecules (up to the maximum value of 1) [10]. Förster and Dexter energy transfer from the host to the guest molecules, and/or direct electron–hole recombination on the guest molecules are the primary mechanisms for achieving high electroluminescence (EL) quantum efficiencies in MOLEDs using a host–guest system in their emitting layer. However, this process complicates the device fabrication and may result in higher operating voltages if the dopant acts as a charge carrier trap.

Recently, silole or silacyclopentadiene derivatives have been proposed as a new class of electron transporting and highly fluorescent materials that can be used in their neat forms in MOLEDs [11–14]. Silole is a silicon-substituted cyclopentadiene with strong electron-accepting properties. The large electron affinity (and therefore low-lying lowest unoccupied molecular orbitals (LUMO)) is attributed to the σ^*–π^* conjugation between the σ^* orbital of the two exocyclic Si–C σ-bonds and the π^* orbital of the butadiene moiety on the silole ring [11,12]. This interaction results in lowering the position of the LUMO level and suggests that siloles have the potential to serve as good electron transport materials. Murata et al. have shown that a silole derivative, namely 2,5-bis(2′,2″-bipyridin-6-yl)-1,1-dimethyl-3,4-diphenylsilacyclopentadiene (PyPySPyPy), exhibits non-dispersive electron transport with a high mobility of 2×10^{-4} cm^2/V s at 0.64 MV/cm in either nitrogen or air [13]. Using PyPySPyPy in the electron transport layer and a highly luminescent silole derivative, namely 1,2-bis(1-methyl-2,3,4,5,-tetraphenylsilacyclopentadienyl)ethane (2PSP) as the emitter with *N*,*N*′-diphenyl-*N*,*N*′-bis(3-methylphenyl)-1,1′-biphenyl-4,4′diamine (TPD) as the hole transporting layer, an EL quantum efficiency of 4.8% was achieved [14].

Here, the performance of MOLEDs using 1,2-bis(1-methyl-2,3,4,5,-tetraphenylsilacyclopentadienyl)ethane (2PSP), 2,5-di-(3-biphenyl)-1,1-dimethyl-3,4-diphenylsilacyclopentadiene (PPSPP) and a new green, highly fluorescent silole derivative, namely 9-silafluorene-9-spiro-1′-(2′,3′,4′,5′-tetraphenyl)-1′H-silacyclopentadiene (ASP), as emissive materials with 2,5-bis(2′,2″-bipyridin-6-yl)-1,1-dimethyl-3,4-diphenylsilacyclopentadiene (PyPySPyPy) and *N*,*N*′-diphenyl-*N*,*N*′-(2-napthyl)-(1,1′-phenyl)-4,4′-diamine (NPB) or *N*,*N*′-diphenyl-*N*,*N*′-bis(3-methylphenyl)-1,1′-biphenyl-4,4′diamine (TPD) as the electron and hole transporting materials, respectively, is reported. A low operating voltage of $\sim$4–4.5 V was measured at a luminance of 100 cd/m^2 and high external EL quantum efficiencies of 3.4–4.1% were obtained at $\sim$100 A/m^2.

2. Experimental details

The silole derivatives were synthesized by a one-step process from bis(phenylethynyl)silanes based on the intermolecular reductive cyclization followed by the palladium-catalyzed cross-coupling with aryl halide [11]. They were purified by recrystallization, column chromatography and vacuum sublimation. They form polycrystalline films upon vacuum evaporation with relatively high glass transition temperatures ($\sim$85 °C). The molecular structures of the siloles derivatives and the hole transporting materials along with the two device structures used in this work are shown in Fig. 1. Both TPD and NPB were purchased from H.W. Sands Corp. and used as received.

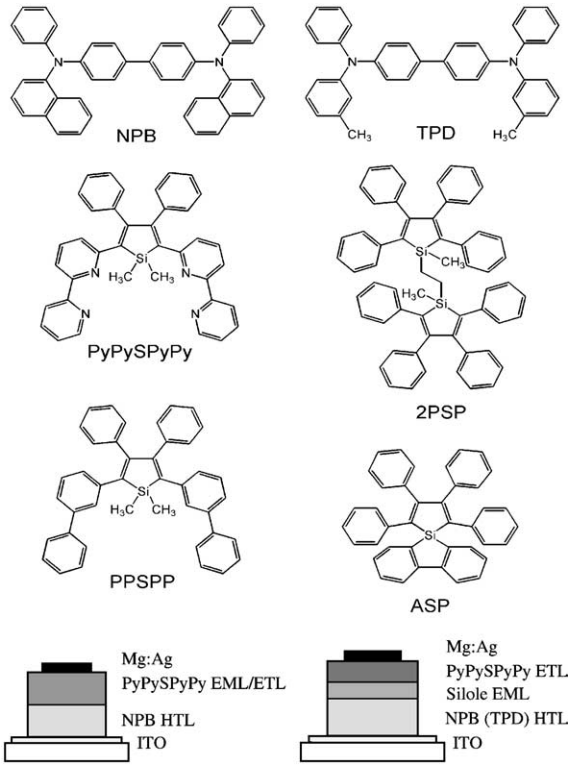

Fig. 1. Device structures and chemical structures of materials used in this work.

Multilayer light-emitting diodes were prepared in a vacuum chamber at low pressure ($\sim 5 \times 10^{-7}$ Torr). Indium tin oxide (ITO) patterned glass substrates were cleaned sequentially in detergent, deionized water, acetone and isopropanol in an ultrasonic bath, and finally were subjected to oxygen plasma treatment for 5 min. A 50 nm thick film of NPB or TPD was first deposited onto ITO and used as a hole transport layer (HTL). A 40–50 nm thick film of PPSPP, 2PSP or ASP was typically used as the emitting layer (EML) with an additional 10–20 nm thick film of PyPySPyPy used as the electron transport layer (ETL). In bilayer devices, where PyPySPyPy was used as the EML/ETL, its thickness was ~60 nm. The total thickness of the organic layers is estimated to be ~110 nm. The deposition rate (typically 0.1–0.3 nm/s) was monitored by an in situ quartz crystal microbalance and used to estimate the thickness of each of the deposited layers. A 150 nm thick Mg:Ag cathode, prepared by coevaporation of Mg and Ag at a weight ratio of 10 to 1, was then deposited onto the organic layers through a shadow mask. 200–300 nm thick films of the silole derivatives were also vacuum deposited on glass substrates for spectroscopic characterization. Absorption spectra were recorded with a HP 8453 UV–vis spectrophotometer. All optical and electrical characterization was performed inside a dry nitrogen-filled glove box, containing <1 ppm concentrations of oxygen and water. Photoluminescence and electroluminescence spectra were recorded with a 270M Spectrograph (from ISA/Spex) coupled to a liquid nitrogen cooled CCD camera, with the samples excited by the 325 nm line of a HeCd laser for the PL measurements. The angular dependence of the EL spectra was measured with a rotating stage on which the devices were mounted. Absolute photoluminescence quantum yields of vacuum-deposited silole films were measured using an integrating sphere, inside the glove box, coupled via a fiber optic link to a monochromator with a CCD camera as the detector. The films were mounted inside the sphere and excited at 325 nm. Current–voltage and luminance–voltage measurements were performed using a Keithley 238 source measurement unit and a Minolta LS-110 calibrated luminance meter, respectively. The device external EL quantum efficiencies, defined as the ratio of the emitted photons to the number of injected electrons, were calculated as the measured ratio of the device luminance to the current density, taking into account the EL device spectrum, the angular dependence of the EL intensity and the eye photopic spectral response function. Small deviations of the measured EL intensities from a Lambertian emission pattern that assumes isotropic emission from light-emitting dipoles inside the emitting layer, were observed at different angles. We attribute this effect to weak wide angle optical interference effects in the presence of the highly reflective cathode metal mirror. A correction factor of ~1.2, derived from the emitted EL intensity in all directions, was used to accurately determine the device EL quantum efficiencies.

3. Results and discussion

3.1. Spectroscopic characterization of the silole derivatives and their exciplexes

3.1.1. Absorption spectra

Fig. 2 shows the absorption spectra of pristine films of 2PSP, ASP, PyPySPyPy and PPSSP. The absorption spectra of polycrystalline films of all the siloles have their main absorption bands in the UV–visible region, depending on the nature of the 2,5-diaryl groups. These broad absorption bands are ascribed to the π–π^* transition of the silole π-conjugated moieties. The first absorption maximum of PyPySPyPy is centered around 391 nm, red-shifted by approximately 27 nm compared to the maximum of PPSPP around 364 nm. This effect is attributed to an extension of the π-conjugation length by substituting the phenyl groups of PPSPP with the electron withdrawing bipyridyl groups in PyPySPyPy. The extension of conjugation is, however, not very effective as it is demonstrated by the very similar bandgaps of the two siloles determined at the edge of the onset of absorption. This is due to the steric hindrance effects that exist between the silole ring and the 2,5-diaryl groups which generally result in a non-planar molecular conformation. The first absorption maximum of 2PSP exhibits a ~28 nm hypsochromic blue shift compared with that of PyPySPyPy resulting in a ~0.1 eV larger bandgap for 2PSP. This is attributed to the non-planar geometry of the 2PSP molecule where the two silole rings are connected by an ethyl linkage resulting in a reduced π-conjugation. The main absorption band of ASP exhibits a maxima around 385 nm.

3.1.2. Fluorescence spectra

Films of PPSPP, 2PSP, ASP and PyPySPyPy exhibit blue to greenish blue to green fluorescence in the solid state. The PL spectra of films of PyPySPyPy, PPSPP, 2PSP and ASP are depicted in Fig. 3. The PL spectrum of PPSPP shows blue emission with a peak at 476 nm. The peak emission of PyPySPyPy is at 505 nm, showing a ~30 nm red-shift relative to that of PPSPP. Substitution of the electron donating phenyl in PPSPP with the strong electron withdrawing bipyridyl group in PyPySPyPy resulted in an increase in the π-electron delocalization which caused the red-shifting of the PyPySPyPy emission spectrum. The PL spectra of 2PSP and ASP exhibit emission maxima around 495 and 525 nm, respectively.

In Fig. 3, the PL spectra of films of NPB:PyPySPyPy and NPB:PPSPP composites are also shown. Interestingly, both the PL spectra of the composite films of NPB and PyPySPyPy or PPSPP are red-shifted relative to those of pristine films of PyPySPyPy and PPSPP. The PL spectrum of the NPB:PyPySPyPy composite film has a peak at 550

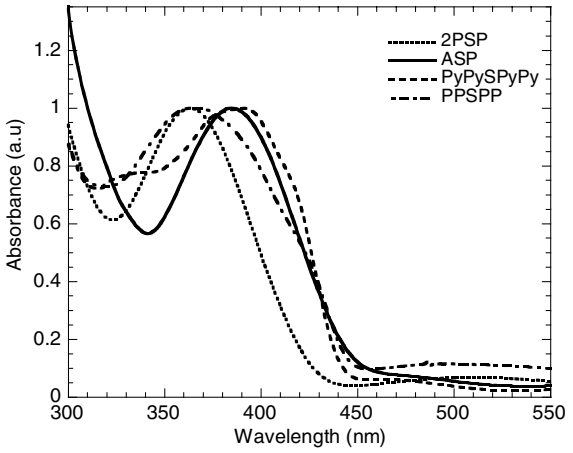

Fig. 2. Optical absorption spectra of thin films of 2PSP, ASP, PyPySPyPy and PPSSP.

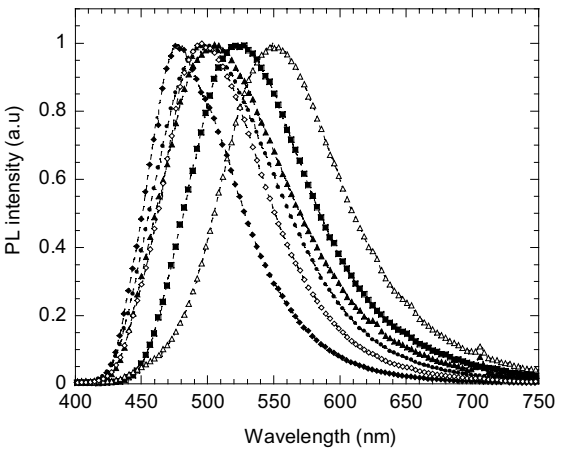

Fig. 3. PL spectra of 2PSP (●), ASP (■), PyPySPyPy (▲), PPSPP (◆), NPB:PyPySPyPy (△) and NPB:PPSPP (◇).

nm, red-shifted by ~45 nm relative to that of PyPySPyPy. Similarly, the PL spectrum of the NPB:PPSPP composite film is centered at 495 nm, red-shifted by ~20 nm relative to that of PPSPP. These red-shifted PL spectra are attributed to excited state complexes (exciplexes) formed between the electron donor (NPB) and the electron acceptor (PPSPP or PyPySPyPy), respectively [15–17]. Exciplex formation can occur due to the relatively large difference between the HOMO and LUMO energy levels of the donor and acceptor molecules. The HOMO energy level of both PPSPP and PyPySPyPy, as measured by ultraviolet photoemission spectroscopy, is ~5.9 eV. The LUMO energy levels of PPSPP and PyPySPyPy were estimated to be ~3.1 and 3.2 eV, respectively, using their optical band gaps determined from the absorption onset. [2] The LUMO level is slightly lowered by ~0.1 eV upon substitution of the phenyl group with the π-electron deficient bipyridyl group. For NPB, the corresponding values of the HOMO and LUMO are 5.5 and 2.4 eV, respectively [18]. The energy of the exciplex is related to the energy difference between the HOMO of the electron donor and the LUMO of the electron acceptor. Ignoring Coulombic attraction between the donor and acceptor, the peak photon energy of the exciplex is estimated from the difference between the ionization potential of the hole transporter and the electron affinity of the electron transporter to be ~2.4 and 2.3 eV for the NPB:PPSPP and NPB:PyPySPyPy exciplexes, respectively. These values are in good agreement with the experimentally derived value of ~2.5 and 2.4 eV, obtained from the PL spectra of the composite films. In contrast, no evidence for exciplex formation between NPB and 2PSP or ASP was found as it is suggested by the almost identical shape and peak emission maxima of the PL spectra of composites of NPB and 2PSP or ASP with the fluorescence spectra of 2PSP and ASP, respectively (not shown here).

[2] A zero exciton binding energy was assumed in estimating the LUMO level from the optical bandgap deduced from the onset of the absorption. The transport gap which is more relevant to carrier injection is equal to the optical gap plus the exciton binding energy.

The absolute PL quantum yields of the NPB:PPSPP and NPB:PyPySPyPy films were measured and are ~0.62 and 0.21, respectively [15]. The absolute PL quantum yields of neat films of 2PSP, ASP, PPSPP and PyPySPyPy were also measured and are (0.94 ± 0.05), (0.87 ± 0.05), (0.85 ± 0.05) and (0.28 ± 0.03), respectively. The PL quantum efficiencies of both exciplexes are slightly lower than those of the respective siloles suggesting that the lifetimes of the silole excited states and those of the corresponding exciplexes are similar. This may further indicate that the excited state complex between the two molecules retains a "silole excited state" character. It is worth noting that the PL quantum yield of NPB:PPSPP is the highest reported for exciplex emission and that the PL quantum yields of the three siloles are among the highest reported for neat organic films. The significant decrease of the PL efficiency of PyPySPyPy compared to PPSPP upon substitution of the phenyl with the bipyridyl groups may be attributed to a more planar geometry of PyPySPyPy. This geometry can result in increased close packing of the molecules in the solid state giving rise to significant intermolecular interactions and quenching of the luminescence. Alternatively, strong vibronic couplings may occur between the silole ring and the bipyridyl group leading to new non-radiative decay pathways.

3.1.3. Electroluminescence spectra

Fig. 4 depicts the EL spectra of bilayer devices based on PyPySPyPy as the EML/ETL and three-layer devices based on PyPySPyPy as the ETL and 2PSP, ASP or PPSPP as the EML, respectively. The EL spectra of the devices based on PPSPP and PyPySPyPy as the emitters are similar to the PL spectra of the NPB:PPSPP and NPB:PyPySPyPy composite films suggesting the formation of an exciplex at the interface between NPB and PPSPP or PyPySPyPy. The weak shoulder around 450 nm in the EL spectra of the bilayer devices is due to a contribution from NPB which indicates that electron–hole recombination partially occurs inside the NPB layer. Indirect carrier recombination may take place between NPB and PPSPP or PyPySPyPy resulting in the formation of an exciplex with a red-shifted featureless EL spectrum [15–17].

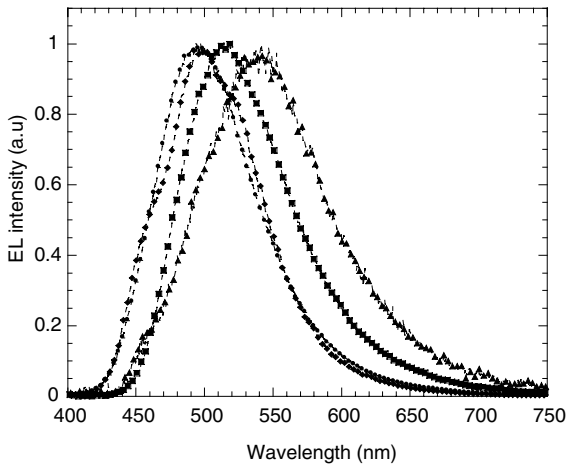

Fig. 4. EL spectra of bilayer devices based on PyPySPyPy as the EML/ETL (▲) and three-layer devices based on PyPySPyPy as the ETL and 2PSP (●), ASP (■) or PPSPP (◆) as the EML, respectively.

In contrast, the EL spectra of devices based on 2PSP and ASP are almost identical to the PL spectra of the respective siloles (their EL emission maxima are at 495 and 525 nm, respectively) which indicates that the same silole excited state (no exciplex) is formed under either photoexcitation or carrier injection.

Considering the similar energetics at the interfaces between NPB and each of the siloles (the HOMO level of 2PSP is ~6.0 eV and the LUMO level is ~3.1 eV which are almost identical to the corresponding levels of PPSPP and PyPySPyPy), it may at first seem rather surprising that only two of the silole derivatives, namely PyPySPyPy and PPSPP, appear to form exciplexes with NPB. One possible explanation may be derived from the significant steric hindrance effects that would result from the more non-planar geometries of 2PSP and ASP, which would not allow the formation of an excited state complex with NPB. The probability to form an exciplex is generally thought to be related to the relative orientation and position of the constituent molecules as exciplex formation requires small interplanar distances between the donor and acceptor molecules with their molecular planes being close to align parallel to each other [19]. Hence, it may be more difficult for 2PSP and ASP to be in a parallel geometry with regard to the plane of the NPB molecule in the excited state, thus preventing exciplex formation.

3.2. Device characterization

Three-layer devices with either NPB or TPD as the HTL, 2PSP, ASP or PPSPP as the EML and PyPySPyPy as the ETL were fabricated and characterized. Fig. 5 shows plots of the current density and luminance as a function of the applied voltage for this series of devices. Three-layer devices using PyPySPyPy as the ETL and 2PSP, ASP or PPSPP as the EML exhibit very low turn-on and operating voltages as well as high luminances. All three-layer devices exhibit rather similar current density–voltage characteristics that follow the current density–voltage characteristics of bilayer devices with PyPySPyPy as the EML/ETL [17]. In multilayer MOLEDs, as the current voltage characteristics are influenced by the injection and transport of both electrons and holes, better electron transport and/or injection is expected to result in a lower operating voltage. In these devices, the hole injection barrier at the ITO/NPB interface is estimated to be ~0.5 eV [18] while the electron injection barrier at the PyPySPyPy/Mg interface is assumed to be relatively small [20,21]. Assuming similar charge injection efficiencies at the anode

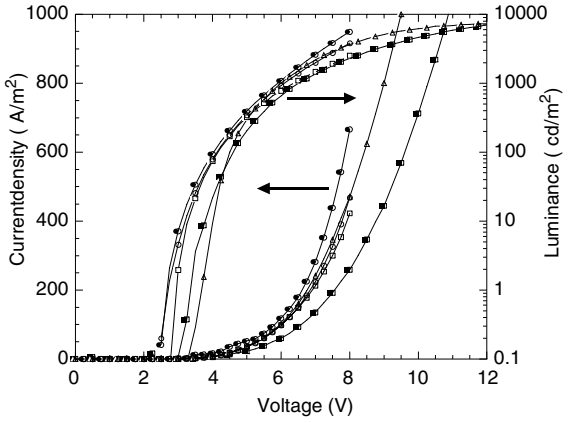

Fig. 5. Current density–voltage–luminance characteristics for three-layer devices: (a) NPB/2PSP/PyPySPyPy (■), (b) NPB/ASP/PyPySPyPy (●), (c) NPB/PPSPP/PyPySPyPy (△), (d) TPD/2PSP/PyPySPyPy (□) and (e) TPD/ASP/PyPySPyPy (○).

and cathode, respectively, charge transfer at the internal interfaces and charge transport are expected to significantly influence the current flow and device efficiency. Therefore, by using an excellent electron transporter (PyPySPyPy) with a low-lying LUMO level adjacent to the cathode, that results in a small electron injection barrier, electron injection and transport to the silole EML will be facilitated resulting in low turn on and operating voltages. The alignment of the silole LUMO levels is further expected to facilitate electron transfer at the 2PSP, ASP or PPSPP/PyPySPyPy interface, increasing the charge recombination/exciton formation rate within the silole EML. The internal barrier of ~0.5 eV for hole transfer at the NPB/silole EML interface will also result in hole accumulation at this interface and electric field redistribution inside the device in order to establish balanced injection. Screening of the electric field due to the internal hole space charge is expected to result in a larger electric field drop across the PyPySPyPy/cathode interface and enhanced electron injection. As the injection and transport of electrons will mainly dictate the luminance turn on voltage for these devices, the similarity between the turn on voltages for the three devices suggests that the electron transfer rate at the silole/PyPySPyPy interface is similar for 2PSP, PPSPP and PyPySPyPy. Luminances of 100 cd/m^2 are achieved at 4.0, 4.5 and 4.6 V for devices based on ASP, PPSPP and 2PSP, respectively when NPB is used as the HTL. A luminance of 1000 cd/m^2 was obtained at 5.9, 6.0 and 6.5 V for devices based on ASP, PPSPP and 2PSP, respectively. (In comparison, bilayer devices with a 2PSP or PPSPP EML/ETL reach a luminance of 100 cd/m^2 at 6.0 and 6.6 V, respectively, and show much lower maximum luminances [17].) The high luminance values observed in three-layer devices are attributed to the high overall exciton recombination rate and the improved exciton confinement within the highly emissive 2PSP, ASP and PPSPP layers as a result of the improved electron injection/transport due to PyPySPyPy and the alignment of the LUMO levels at the silole/PyPySPyPy interface. Maximum luminances of 7000–10,000 cd/m^2 were achieved for the silole based three-layer devices.

In Figs. 6 and 7, plots of the external EL quantum efficiency and the luminous power efficiency are presented as a function of current density and luminance, respectively. All the three-layer devices exhibit high external EL quantum and luminous power efficiencies for a wide range of current densities and brightness. The external EL quantum efficiency reaches a maximum of 3.8%,

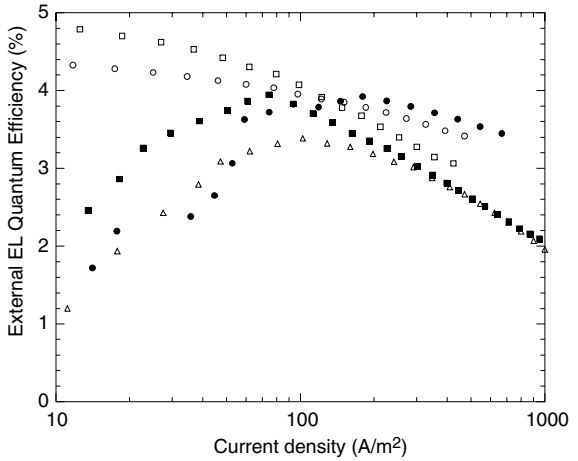

Fig. 6. External EL quantum efficiency versus current density for three-layer devices: (a) NPB/2PSP/PyPySPyPy (■), (b) NPB/ASP/PyPySPyPy (●), (c) NPB/PPSPP/PyPySPyPy (△), (d) TPD/2PSP/PyPySPyPy (□) and (e) TPD/ASP/PyPySPyPy (○).

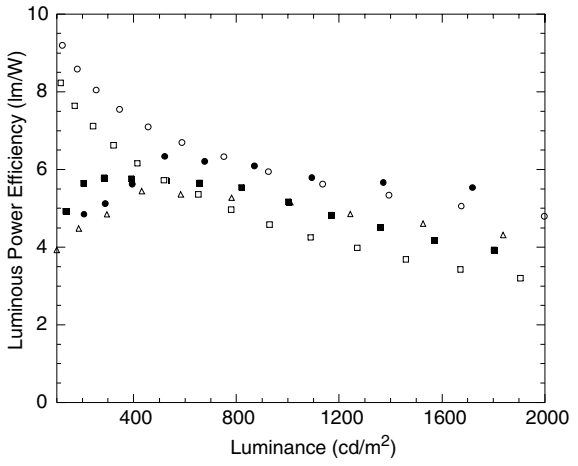

Fig. 7. Luminous power efficiency versus luminance for three-layer devices: (a) NPB/2PSP/PyPySPyPy (■), (b) NPB/ASP/PyPySPyPy (●), (c) NPB/PPSPP/PyPySPyPy (△), (d) TPD/2PSP/PyPySPyPy (□) and (e) TPD/ASP/PyPySPyPy (○).

3.9% and 3.4% for ASP, 2PSP and PPSPP, respectively (at ~100 A/m^2) when NPB is used as the HTL. At 1000 A/m^2, the EL quantum efficiencies are 2.1% and 2% for 2PSP and PPSPP, respectively. (In comparison, bilayer devices have lower EL quantum efficiencies that reach a maximum of 2.2% for 2PSP and 1% for PPSPP at ~100 A/m^2 [17].) The luminous power efficiencies of PPSPP devices based on exciplex emission are 4.0 and 5.2 lm/W at 100 and 1000 cd/m^2, respectively. Devices based on 2PSP and ASP exhibit power efficiencies of 4.6 and 5.2 lm/W, respectively, at 100 cd/m^2. At 1000 cd/m^2, power efficiencies of 5.2 and 5.9 lm/W are achieved for 2PSP and ASP devices, respectively. All silole-based devices show a peak of the EL quantum efficiency at current densities of ~100 A/m^2 with a gradual decrease at higher current densities. It is worth noting that the EL quantum efficiency of the ITO/NPB/PPSPP/PyPySPyPy/Mg:Ag three-layer MOLEDs is the highest ever reported based on exciplex emission arising at the interface of an emitter (PPSPP) and a hole transporter (NPB) [16]. The very high EL quantum efficiencies of these silole based MOLEDs is attributed to the use of the high electron mobility PyPySPyPy as the ETL with improved electron transport, thus reducing electron accumulation and non-radiative exciton recombination at the cathode, and to an increasing carrier recombination efficiency and a higher overall exciton generation rate due to the improved charge balance. We note that electron-only devices based on PyPySPyPy with symmetric Mg:Ag contacts were shown to exhibit a higher electron current flow compared to those using either 2PSP or PPSPP, suggesting a higher conductivity for the PyPySPyPy solid film [21]. The very high Φ_{PL} of the neat silole films and the exciplex further contributes to the very high efficiency of these MOLEDs. The effect of varying the emitting layer thickness on the device performance was also examined in a three-layer device configuration with a TPD HTL. Devices with a 20 nm thick 2PSP or ASP layer and a ~30 nm thick PyPySPyPy layer show improved performance with operating voltages of ~4.0 V and EL quantum efficiencies of 4.1% (8.5 lm/W at 100 cd/m^2) and 4.0% (9.6 lm/W at 100 cd/m^2) at 100 A/m^2. Maximum EL quantum efficiencies of 4.8% and 4.3% for the 2PSP and ASP-based devices were obtained at ~10 A/m^2. The improved EL quantum efficiencies (particularly at lower voltages) and the slightly lower operating voltages can be attributed to the excellent confinement of the recombination zone within the thin emissive silole layer and the lower barrier for hole injection at the ITO/TPD interface. A summary of the three-layer device characteristics is presented in Table 1.

The external EL quantum efficiency η_{EL} of MOLEDs is given by

$$\eta_{EL} = \alpha\gamma\eta_r\Phi_{PL}, \quad (1)$$

where α is the light output coupling factor ($\alpha = 1/(2n^2)$, where n is the refractive index of the emissive medium), γ is the charge carrier balance factor (which determines the charge recombination probability and the exciton generation rate), η_r is the generation efficiency of singlet excitons and Φ_{PL} is the absolute PL quantum efficiency of the emitter. It is important to note that the external EL quantum efficiency for all the silole based MOLEDs approaches the theoretical limit of ~5% for fluorescent emitters with a PL quantum efficiency of ~100%. This estimate of the theoretical limit is based on a light output coupling factor of

Table 1
Comparison of the driving voltages, external EL quantum and luminous power efficiencies of three-layer devices with NPB or TPD as HTL, 2PSP, ASP or PPSPP as EML and PyPySPyPy as ETL

HTL/EML	Driving voltage (V) (at 100 cd/m^2)	External EL quantum efficiency (%) (at 100 A/m^2)	Luminous power efficiency (lm/W) (at 100 cd/m^2)
NPB/2PSP	4.6	3.8	4.6
NPB/ASP	4.0	3.8	5.2
NPB/PPSPP	4.5	3.4	4.0
TPD/2PSP	4.1	4.1	8.5
TPD/ASP	4.1	4.0	9.6

~0.2, a maximum carrier recombination efficiency of ~1 and singlet excitons' formation probability of ~0.25 (assuming spin statistics is preserved). The near-perfect charge recombination efficiency and the close to unity PL quantum efficiencies of the siloles suggest that further improvements in device efficiency could be realized mainly by employing novel light outcoupling schemes. The very high Φ_{PL} of the siloles can therefore result in excellent device performance without the use of highly fluorescent or phosphorescent dopants when optimized device architectures are employed.

4. Conclusions

In summary, we have reported the performance of highly efficient fluorescent MOLEDs based on a new class of highly emissive silole derivatives. Three-layer devices with PPSPP, 2PSP and ASP as emissive layers and PyPySPyPy as the electron transport layer exhibit low operating voltages of ~4–4.5 V and high EL quantum efficiencies of 3.4–4.8%. PPSPP and PyPySPyPy were also found to form exciplexes with the hole transporting NPB and TPD molecules. The use of the high electron mobility PyPySPyPy electron transporter combined with the highly efficient silole emitters in a three-layer device configuration with a hole transporter enabled us to demonstrate high performance MOLEDs that emit nearly blue to green light.

Acknowledgements

The authors thank Dr. Antti Mäkinen at NRL for conducting UPS measurements on the siloles and the Office of Naval Research for financial support of this work.

References

[1] C.W. Tang, S.A. Van Slyke, Appl. Phys. Lett. 51 (1987) 913.
[2] F. Steuber, J. Staudigel, M. Stössel, J. Simmerer, A. Winnacker, H. Spreitzer, F. Weissörtel, J. Salbeck, Adv. Mater. 12 (2000) 130.
[3] J.S. Huang, M. Pfeiffer, A. Werner, J. Blochwitz, K. Leo, S.Y. Liu, Appl. Phys. Lett. 80 (2002) 139.
[4] M. Pfeiffer, S.R. Forrest, K. Leo, M.E. Thompson, Adv. Mater. 14 (2002) 1633.
[5] A.R. Duggal, J.J. Shiang, C.M. Heller, D.F. Foust, in: Z.H. Kafafi, H. Antoniadis (Eds.), Organic Light Emitting Materials and Devices VI, SPIE Proc. 4800 (2003) 62.
[6] G.E. Jabbour, B. Kippelen, N.R. Armostrong, N. Peyghambarian, Appl. Phys. Lett. 73 (1998) 1185.
[7] G.G. Malliaras, Y. Shen, D.H. Dunlap, H. Murata, Z.H. Kafafi, Appl. Phys. Lett. 79 (2001) 2582.
[8] J. Kido, Y. Izumi, Appl. Phys. Lett. 73 (1998) 2721.
[9] M.A. Baldo, D.F. O'Brien, Y. You, A. Shoustikov, S. Silbley, M.E. Thompson, S.R. Forrest, Nature 395 (1998) 151.
[10] H. Mattoussi, H. Murata, C.D. Merritt, Y. Iizumi, J. Kido, Z.H. Kafafi, J. Appl. Phys. 86 (1999) 2642.
[11] K. Tamao, M. Uchida, T. Izumizawa, K. Furukawa, S. Yamaguchi, J. Am. Chem. Soc. 118 (1996) 11974.
[12] S. Yamaguchi, T. Endo, M. Uchida, T. Izumizawa, K. Furukawa, K. Tamao, Chem. Eur. J. 6 (2000) 1683.
[13] H. Murata, G.G. Malliaras, M. Uchida, Y. Shen, Z.H. Kafafi, Chem. Phys. Lett. 339 (2001) 161.
[14] H. Murata, Z.H. Kafafi, M. Uchida, Appl. Phys. Lett. 80 (2002) 189.
[15] L.C. Palilis, H. Murata, A.J. Mäkinen, M. Uchida, Z.H. Kafafi, Mater. Res. Soc. Proc. 725 (2002) 19.
[16] L.C. Palilis, A.J. Mäkinen, M. Uchida, Z.H. Kafafi, Appl. Phys. Lett. 82 (2003) 2209.
[17] L.C. Palilis, A.J. Mäkinen, H. Murata, M. Uchida, Z.H. Kafafi, in: Z.H. Kafafi, H. Antoniadis (Eds.), Organic Light Emitting Materials and Devices VI, SPIE Proc. 4800 (2003) 256.
[18] Q.T. Le, E.W. Forsythe, F. Nuesch, L.J. Rothberg, L. Yan, Y. Gao, Thin Solid Films 363 (2000) 42.
[19] J. Kalinowski, M. Cocchi, P. Di Marco, V. Fattori, Chem. Phys. Lett. 318 (2000) 137.
[20] A.J. Mäkinen, M. Uchida, Z.H. Kafafi, Appl. Phys. Lett. 82 (2003) 3889.
[21] L.C. Palilis, M. Uchida, Z.H. Kafafi, IEEE J. Sel. Top. Quantum Electron. 9 (6) (2003).